

Surface Modification of Low-Density Polyethylene by Inductively Coupled Argon Plasma

S. Tajima and K. Komvopoulos*

Department of Mechanical Engineering, University of California, Berkeley, California 94720

Received: April 23, 2005; In Final Form: June 16, 2005

The surface chemistry and nanotopography of low-density polyethylene (LDPE) were modified by downstream, inductively coupled, radio frequency (rf) Ar plasma without inducing surface damage. The extent of surface modification was controlled by the applied ion energy fluence, determined from the plasma ion density measured with a Langmuir probe. The treated LDPE surfaces were characterized by atomic force microscope (AFM) imaging, contact angle measurements, and X-ray photoelectron spectroscopy (XPS). Analysis of AFM surface images confirmed that topography changes occurred at the nanoscale and that surface damage was insignificant. Contact angle measurements demonstrated an enhancement of the surface hydrophilicity with the increase of the plasma power. XPS results showed surface chemistry changes involving the development of different carbon–oxygen functionalities that increased the surface hydrophilicity. Physical and chemical surface modification was achieved under conditions conducive to high-density inductively coupled rf plasma.

Introduction

Low-density polyethylene (LDPE) is used in various electrical, coating, printing, bonding, and biomedical applications.¹ A fundamental requirement is the strong adhesion of LDPE to various metal and polymer surfaces, fibers, and print dye. However, the bond strength to most materials is rather weak because the surface of LDPE is nonpolar. Thus, treatments to increase the surface energy of LDPE^{2,3} by introducing polar functionalities (e.g., alcohol, ether, carbonyl, ester, and carboxyl polar groups)⁴ are desirable. It is important that these treatments are surface specific so that the bulk properties are preserved.

Different bulk and surface treatments, such as γ -ray⁵ and electron beam⁶ irradiation, chromic acid,^{7,8} corona discharge,⁹ and different plasma methods^{10–14} have been used to improve adhesion and biocompatibility. γ -ray and electron beam irradiation are bulk treatments that are not surface specific. Chromic acid is a wet process that requires handling and disposal of harmful chemicals. Although corona discharge is a surface treatment, it is not suitable for three-dimensional objects and produces significant changes in the surface topography.^{15,16} Plasma treatment has the advantage over previous methods that modification is confined within the surface layer of the material.^{12–14} In addition, thermal degradation is minimal because the process temperature is low and treatment is fast, clean, environmentally safe, and uniform even for components with complex shapes.

Plasma gas plays a dominant role in the modification process of the polymer surface. Oxygen plasma has been used to produce various functional groups on LDPE surfaces.^{4,10,11,14} Although this treatment promotes the formation of polar functionalities, it causes chain scission which is a precursor to the rapid degradation of the polymer surface.^{17,18} As an alternative, exposure to inert plasma (e.g., Ar and He) can be used to produce polar functionalities on polymer surfaces. Oxygen from the ambient has been detected on polymer surfaces treated with Ar plasma.^{13,19,20} This is attributed to the attachment of atomic

oxygen to radicals at the polymer surface resulting from the abstraction of hydrogen atoms by bombarding Ar ions.^{17,21} X-ray photoelectron spectroscopy (XPS) results have shown the presence of alcohol and ether groups on polymer surfaces treated with Ar plasma.²⁰

The main polar functionalities on LDPE surfaces exposed to capacitively coupled Ar plasma and, subsequently, to ambient air have been reported to be alcohol and/or ether,²⁰ and small amounts of carbonyl;²² however, carboxyl groups were not detected in the former studies. It is likely that polar functionalities produced from oxygen plasma treatment could be obtained with intense Ar plasma treatment followed by exposure to the atmosphere. This hypothesis was evaluated in this study, which was aimed to examine whether polar functionalities responsible for high surface adhesion can be produced by energetic Ar plasma treatment without the undesirable effect of chain scission occurring during oxygen plasma treatment.

Capacitively coupled plasma (CCP) was used in several earlier studies to treat LDPE surfaces.^{4,10,11,14,20} Inductively coupled plasma (ICP) is more advantageous than CCP because process control is easier and the power and ion density ranges are broader. In addition, ICP produces higher ion densities and lower voltage across the sheath than CCP.²³ These characteristics of ICP are especially desirable in polymer surface treatments. High ion densities can yield sufficiently high ion energies for surface chemical modification, while the low sheath voltage reduces surface damage by the impinging ions. To minimize surface damage resulting from ion bombardment,²⁴ it is advantageous to place the polymer samples downstream from the ICP power source.

The main objective of this investigation was to explore whether polar functional groups can be produced on LDPE surfaces by ICP discharge without surface damage. Atomic force microscope (AFM), contact angle, and XPS results are presented to elucidate the evolution of the surface topography (texture), surface energy, and chemical behavior of LDPE treated with Ar plasma in terms of the ion energy fluence measured in situ with a Langmuir probe.

* Corresponding Author: Telephone: (510) 642-2563. Fax: (510) 643-5599. E-Mail: kyriakos@me.berkeley.edu.

Experimental Procedures

Polyethylene Specimens. Pellets of LDPE (Sigma-Aldrich, St. Louis, MO) were press-casted on AFM metal disks. The LDPE pellets were first heated at 160 °C for 2 min until they became transparent and then pressed against a cleaned glass plate for 3 min while they were maintained at 160 °C to obtain a flat surface. Finally, the LDPE samples were allowed to cool in ambient air for about 1–1.5 min before they were peeled off from the glass plate. The thickness of the LDPE samples was in the range of 800–900 μm .

Plasma Treatment. An inductively coupled, high-density, radio frequency (rf) plasma source (Litmas Inc., Charlotte, NC) was used to generate the plasma. The rf power source (with excitation frequency of 13.56 MHz) includes a variable-frequency power supply and a solid-state matching network to optimize the output power.²⁵ The rf power was varied between 75 and 1200 W with increments of 75 W. To prevent excessive topography changes, downstream plasma was used to treat the LDPE surfaces instead of direct plasma applied when the samples were placed inside the ICP power source. The ion energy fluence was determined from the ion density, which was measured in situ with the Langmuir probe.

The 20.3 cm-diameter main chamber consists of 304 stainless steel and has eight flange ports of 7 cm in diameter for pressure gauges and five flange ports of 3.4 cm in diameter that are used as viewing windows. The aluminum sample holder is connected to a coaxial, grounded shield feed through. The sample holder was placed at a distance of ~ 58 cm from the bottom of the ICP source. The present setting uses three types of pressure gauges—a convecTorr (Varian Vacuum Technologies, Lexington, MA) gauge and a hot filament ionization gauge for low and high vacuum level measurement, respectively, and a capacitance manometer coupled with a pendulum control valve for pressure control. To avoid polymer deposition and to maintain accuracy during processing, the capacitance manometer was heated at 100 °C. During plasma treatment, the chamber pressure was maintained at 500 mTorr. The pumping system consists of a hybrid turbomolecular pump with a vent valve and a rotary-vane backing pump. The base pressure of the main chamber was $\sim 10^{-6}$ Torr. A digital mass flow controller attached to the gas inlet of the power supply was used to control the flow of the plasma gas (99.999% pure Ar from Praxair, Danbury, CT) into the chamber. The flow rate of the Ar gas was set at 100 cm^3/min and was monitored with a computer. Ar gas was introduced into the chamber 5 min before the initiation of the plasma treatment. The duration of each treatment was 15 min. All the treatments were performed within 1–2 h from the fabrication of the polymer samples. A schematic of the experimental set up used to perform the plasma treatments is shown in Figure 1.

Langmuir Probe Measurements. To detect the ion density applied to the sample during plasma treatment, the sample stage was removed and the exposed tip of a cylindrical tungsten probe covered with polyolefin heat shrink was placed at the same position as the sample to be treated. The diameter of the tungsten probe was 0.08 mm and the exposed length of the tip was 6 mm. A negative bias voltage ranging from 0 to -50 V was applied from an external dc voltage supply. The current was calculated from the voltage reading across the external resistor (4.69 k Ω and 210 Ω for power in the ranges of 225–300 and 375–1200 W, respectively). The bias voltage was changed in increments of 3 V, and the voltage across the external resistor was measured four times during a period of 0.5 min. These

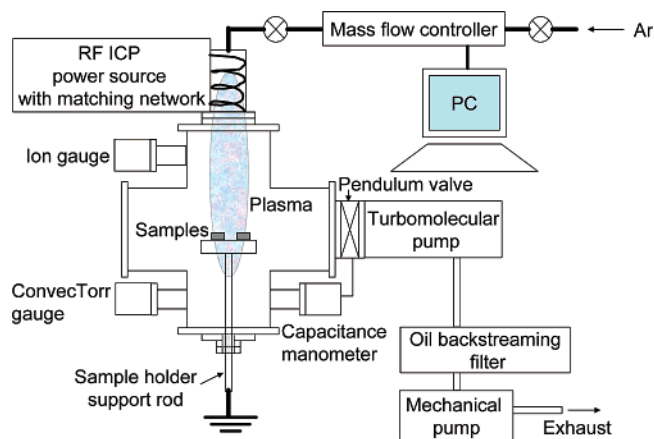


Figure 1. Schematic of the radio frequency inductively coupled plasma system.

voltage readings were first averaged and then converted to current flow through the Langmuir probe.

The ion density at the edge of the plasma sheath n_s was determined from the ion saturation current I_i given by²³

$$I_i = 2en_s r l \left(\frac{2e|\Phi_p - V_B|}{M} \right)^{1/2} \quad (1)$$

where e is the elementary charge (1.6022×10^{-19} C), r is the radius of the probe tip (0.04 mm), l is the exposed tip length (6 mm), Φ_p is the plasma potential, V_B is the applied dc bias voltage, and M is the Ar ion mass (6.7×10^{-26} kg).

Equation 1 shows a linear dependence of the I_i^2 vs $-V_B$ slope on n_s^2 . The $-\partial I_i^2 / \partial V_B$ slope was obtained by applying a linear fit to the I_i^2 vs $-V_B$ curve, and n_s was determined from the relationship

$$n_s = \left(-\frac{\partial I_i^2}{\partial V_B} \right)^{1/2} \left(\frac{M}{2e} \right)^{1/2} \frac{1}{2erl} \approx 5.95 \times 10^{21} \left(-\frac{\partial I_i^2}{\partial V_B} \right)^{1/2} \quad (2)$$

Surface Characterization Methods. The topography, surface energy, and chemical behavior of plasma-treated LDPE were studied in the context of AFM, goniometry, and XPS results. To avoid possible biasing of the measurements resulting from aging effects, the analysis of the specimens using the aforementioned techniques was performed within 0.5–3 h from the plasma treatment.

Surface Topography. Surface characterization of LDPE samples treated with Ar plasma at rf power between 75 and 1200 W was performed with an AFM (Multimode, Nanoscope IV, Veeco Metrology, Santa Barbara, CA). Imaging was carried out in the contact mode using triangular silicon microcantilevers with pyramidal tips of nominal radius of curvature less than 10 nm and stiffness equal to 0.12 N/m. The contact force during scanning was less than 10 nN. Statistical surface roughness parameters, i.e., centerline average (CLA) R_a , root-mean-square (RMS) R_q , skewness S , and kurtosis K , were determined from $1 \mu\text{m} \times 1 \mu\text{m}$, $5 \mu\text{m} \times 5 \mu\text{m}$, and $10 \mu\text{m} \times 10 \mu\text{m}$ AFM surface maps. For statistical analysis, roughness data were calculated as averages of 10 measurements obtained from two or three samples for each plasma treatment.

Goniometry. The hydrophilicity of the surfaces was quantified in terms of static contact angle measurements obtained at room temperature with a drop shape analysis system (DSA10, Krüss GmbH, Hamburg, Germany). Droplets of deionized water (0.2–0.4 μL) were applied to the sample surface with a syringe, and the droplet image was taken within 3 s from application. The

TABLE 1: Ion Density vs Plasma Power

plasma power (W)	ion density (m^{-3})
225	$(8.5 \pm 2.15) \times 10^{12}$
300	$(2.3 \pm 0.92) \times 10^{14}$
375	$(5.9 \pm 0.86) \times 10^{14}$
450	$(1.9 \pm 0.61) \times 10^{15}$
825	$(8.4 \pm 0.99) \times 10^{15}$
1200	$(2.1 \pm 0.37) \times 10^{16}$

angle between the baseline of the droplet and the tangent at the water/air boundary was measured from both sides of the two-dimensional projection of the droplet using the DSA1 software (Krüss GmbH, Hamburg, Germany). To evaluate changes in the polymer hydrophilicity resulting from the plasma treatment, the contact angle was calculated from five different measurements for each sample, using a total of five samples for each plasma treatment, i.e., 25 measurements per treatment.

X-ray Photoelectron Spectroscopy. Both untreated and plasma-treated LDPE samples were characterized by XPS to determine changes in the surface chemistry induced by the Ar plasma. Spectra were obtained with a Perkin-Elmer PHI 5400 ESCA system (without charge neutralization or monochromator) using Al K α (1486.6 eV) X-ray source at 54.7° relative to the analyzer axis. A takeoff angle $\theta = 45^\circ$ measured from the sample surface was used throughout. The sampling depth h is given by⁴

$$h = 3\lambda \sin \theta \quad (3)$$

where λ is the inelastic mean free path (for LDPE, $\lambda = 1.95$ nm).⁴ For $\theta = 45^\circ$ and $\lambda = 1.95$ nm, eq 3 gives $h = 4.1$ nm.

XPS spectra were obtained from 1 mm diameter surface areas using pass energy of 187 and 35.75 eV. The resolution in the survey and detail scans was equal to 1.0 and 0.05 eV, respectively. Relative atomic concentrations were determined from 76.3% Gaussian–23.7% Lorentzian (GL) curve fits using the RBD AugerScan 2 software (RBD Enterprises, Inc., Bend, OR) after Shirley subtraction of the background noise. To compensate for surface charging effects, all binding energies in the core level C 1s spectrum were referenced to the neutral carbon peak centered at 285.0 eV.^{4,7} A full width at half-maximum (fwhm) of 1.46 eV was used for all components of the C 1s spectrum. The fwhm and the peak shape were determined from the averages of 15 multiple C 1s XPS peaks obtained from five untreated LDPE samples.

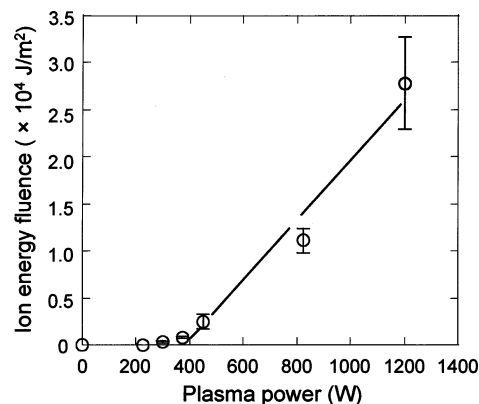
The relative oxygen concentration was calculated based on the method proposed by Wagner.²⁶ From the measured areas under the C 1s and O 1s peaks, denoted by A_C and A_O , respectively, the atomic fraction of oxygen, C_O , was determined from the relationship

$$C_O = \frac{A_O/S_O}{A_O/S_O + A_C/S_C} \quad (4)$$

where S_O and S_C are the sensitivity factors of atomic oxygen and carbon, respectively, with corresponding empirical values equal to 0.711 and 0.296 (quoted from ref 26). For statistical analysis, C_O values were calculated from five to eight C 1s and O 1s spectra obtained from different locations of three or four samples of the same material.

Results and Discussion

Ion Energy Fluence. Ion densities in the range of 10^{12} – 10^{16} m^{-3} were obtained by varying the rf power between 225 and 1200 W. Table 1 gives statistical data of n_s (based on six different measurements) in terms of the plasma power. The ion

**Figure 2.** Ion energy fluence vs plasma power.

energy fluence W (J/m^2) was determined from the measured ion density using the relationship

$$W = eE_i n_s u_B t \quad (5)$$

where E_i is the ion bombarding energy, t is the treatment time (15 min), and u_B is the Bohm velocity given by²³

$$u_B = \left(\frac{eT_e}{M} \right)^{1/2} \quad (6)$$

where T_e ($=E_i/5.2$) is the electron temperature. By equating the total surface particle loss to the total ionization volume,²³ it was found that $T_e = 1.1$ V. Substituting this value in $E_i = 5.2 T_e$ and eq 6 yields $E_i = 5.7$ V and $u_B = 1.6 \times 10^3$ m/s. Since T_e , E_i , and u_B do not depend on the plasma power, they were constant in all the plasma treatments. Substituting the previous values of E_i , u_B , and t into eq 5 yields

$$W \approx 1.3 \times 10^{-12} n_s \quad (7)$$

Figure 2 shows the variation of the ion energy fluence (determined from eq 7 in terms of the measured ion density given in Table 1) with the Ar plasma power. The data reveal the existence of two different discharge regimes. For plasma power less than 400 W, the ion energy fluence was relatively low, while above 400 W it increased linearly with the plasma power. A linear relationship between the plasma power and the ion density above a threshold power has also been observed in a previous study.²⁷ The threshold power represents the critical power level for sustaining an inductive discharge.²³ Below the threshold power, capacitive coupling between the coil and the plasma produces a weakly ionized discharge. The phenomenon of capacitively coupling is a consequence of the longitudinal electric field generated by the voltage drop across the induction coil. When the ion density is low, the plasma is driven capacitively because the highly ionized discharge cannot be sustained by the inductive electric field. Alternatively, when the ion density is high, the discharge is maintained by a circular electric field.²⁸ The data shown in Figure 2 indicate a significant effect of the plasma power on the type of plasma process. The low ion energy fluence obtained with power less than 400 W is a result of the low ion density of the CCP discharge. Alternatively, the high ion density of the ICP discharge is the reason for the significantly higher ion energy generated at power levels above 400 W.

Surface Topography. Representative AFM images of the surface topographies of LDPE treated at different rf power levels are shown in Figure 3. A surface image of the untreated sample is not shown as it was not possible to engage the AFM tip with the polymer surface because of the strong electrostatic charge

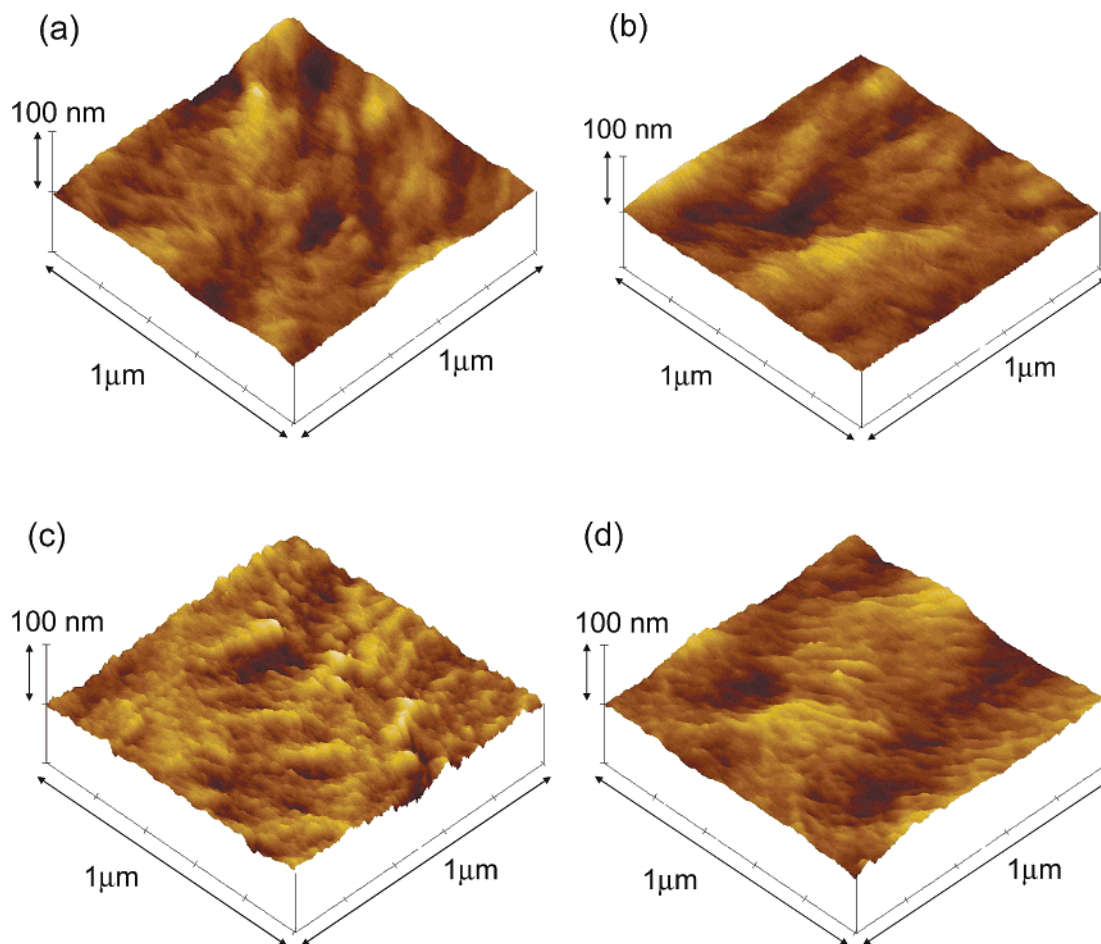


Figure 3. AFM surface images of LDPE for plasma power equal to (a) 75, (b) 225, (c) 450, and (d) 1200 W.

produced when the polymer sample was peeled off from the glass plate. It is presumed that the topography of the LDPE treated at 75 W is similar to that of the untreated polymer. A qualitative comparison of the surface maps shown in Figure 3 shows that the surface morphologies corresponding to the low power treatments (Figures 3a and 3b) do not exhibit discernible differences. However, the LDPE surfaces treated at a relatively high power indicate the occurrence of nanoscale texturing (Figures 3c and 3d), evidently due to the significantly more intense ion bombarding effect resulting from the increase of the ion energy fluence (Figure 2).

To quantify the plasma power (ion energy fluence) effect on the surface topography, statistical roughness parameters were extracted from $1\ \mu\text{m} \times 1\ \mu\text{m}$ AFM images of plasma-treated LDPE surfaces. Figure 4 shows that increasing the plasma power resulted in higher R_a and R_q values; however, the effect on the average S and K values was insignificant. The fact that $S \approx 0$ and $K \approx 3$ regardless of the plasma power indicates that all the surfaces possessed Gaussian asperity distributions. The increase of R_a and R_q is mainly due to nanoscale texturing, resulting from the ICP discharge at power levels above 450 W. Despite the linear increase of the ion energy fluence with the power, additional surface texturing did not occur in the power range of 600–1200 W, implying the existence of a finite power range for surface nanotexturing.

A statistical analysis performed for length scales greater than $1\ \mu\text{m}$ revealed a marginal power effect on surface roughness. Table 2 shows weak power dependence of R_a and R_q obtained from $5\ \mu\text{m} \times 5\ \mu\text{m}$ and $10\ \mu\text{m} \times 10\ \mu\text{m}$ surface scans. In

addition, $S \approx 0$ and $K \approx 3$ throughout the power range examined. Although the general trend is for the roughness to increase with the power, the standard deviation values suggest that the power effect on the microtopography was insignificant. Hence, the statistical surface analysis suggests that, under the present Ar plasma conditions, modification of the surface topography occurred only at the nanoscale and the effect on the surface height distribution was negligible. This nanotexturing effect may be related to differences in the etching rates of the crystalline and amorphous phases present at the LDPE surfaces.

In view of the results shown in Figures 2–4 and Tables 1 and 2, the threshold ion energy fluence (eq 7) for nanotexturing of LDPE under the present experimental setting is estimated to be $2500\ \text{J/m}^2$, corresponding to a plasma power of 450 W. Above this threshold, physical modification of the surface is independent of the ion energy fluence. Hence, downstream ICP discharge minimized the surface damage induced by bombarding Ar ions, yielding only nanoscopic changes in the surface topography of LDPE.

Surface Hydrophilicity. Figure 5 shows (water) contact angle results illustrating the plasma power (ion energy fluence) effect on the hydrophilic behavior of LDPE. The decrease of the contact angle with the increase of the plasma power indicates a change from hydrophobic to hydrophilic surface behavior. The effect is mostly pronounced in the power range of 300–450 W, where the transition from CCP to ICP discharge occurs. The smallest contact angle of $\sim 54^\circ$ was obtained for power higher than 825 W. Similar contact angles (i.e., 45° – 60°) have been reported for LDPE treated with oxygen plasma.²⁹ The compa-

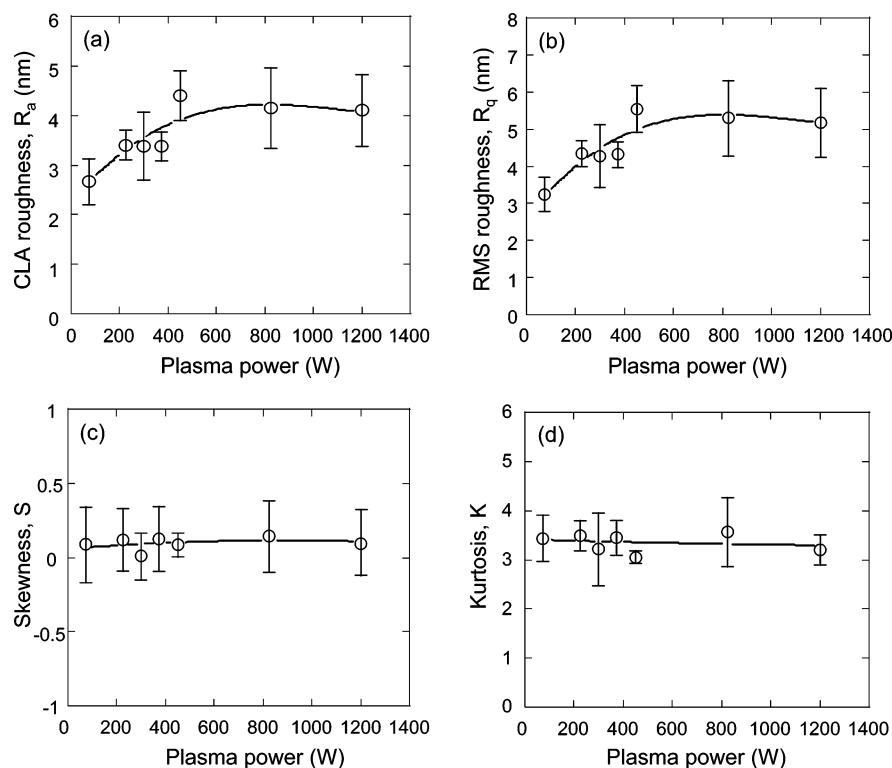


Figure 4. Effect of plasma power on surface roughness of LDPE determined from $1\ \mu\text{m} \times 1\ \mu\text{m}$ AFM surface images: (a) CLA roughness, (b) RMS roughness, (c) skewness, and (d) kurtosis.

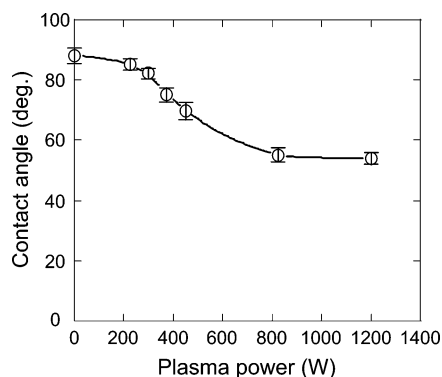


Figure 5. Effect of plasma power on water contact angle of LDPE.

TABLE 2: Surface Roughness Parameters Obtained from $5\ \mu\text{m} \times 5\ \mu\text{m}$ and $10\ \mu\text{m} \times 10\ \mu\text{m}$ AFM Surface Images vs Applied Power Plasma for LDPE Treated with Ar Plasma

plasma power (W)	scan area dimensions			
	$5\ \mu\text{m} \times 5\ \mu\text{m}$		$10\ \mu\text{m} \times 10\ \mu\text{m}$	
	R_a (nm)	R_q (nm)	R_a (nm)	R_q (nm)
75	9.0 ± 1.1	11.5 ± 1.3	15.0 ± 2.3	19.1 ± 2.8
225	9.5 ± 2.3	11.9 ± 2.9	15.9 ± 3.7	20.4 ± 4.6
300	9.0 ± 1.0	11.5 ± 1.3	16.1 ± 0.9	20.5 ± 1.1
375	8.6 ± 1.6	10.9 ± 1.8	14.7 ± 1.7	18.7 ± 1.9
450	9.8 ± 2.0	12.5 ± 2.4	16.1 ± 1.6	20.9 ± 2.0
825	11.1 ± 1.9	14.1 ± 2.3	16.1 ± 1.5	20.6 ± 1.9
1200	11.3 ± 1.4	14.3 ± 1.7	19.1 ± 3.2	24.3 ± 3.7

able contact angle values of LDPE treated with inductively coupled, downstream Ar plasma and oxygen plasma indicate that both treatments produce similar hydrophilic behaviors; however, oxygen plasma induces significant surface damage.

Surface Chemical Composition. The exposure of the plasma-treated LDPE to the ambient yielded relatively high concentrations of polar functionalities on the polymer surfaces. XPS spectra of LDPE treated at different power levels are

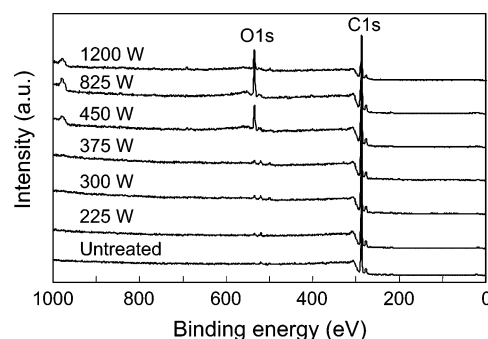


Figure 6. XPS survey spectra for untreated and Ar plasma treated LDPE showing the presence of C 1s (285 eV) and O 1s (533 eV) core level peaks.

compared in Figure 6. The spectra demonstrate the presence of C 1s (285 eV) and O 1s (533 eV) core level peaks and the absence of nitrogen from the ambient or metal contaminants from the sample holder. The increase of the O 1s peak intensity with the increase of the plasma power above 450 W reveals the formation of oxygen-containing functionalities above the $2500\ \text{J/m}^2$ threshold of the ion energy fluence.

Figure 7 shows representative C 1s XPS spectra with GL fits for different power values. All spectra contain a major peak 1 centered at 285 eV which is assigned to C—C and/or C—H bonding. Figure 7a shows that the spectrum of the untreated LDPE contains only peak 1. This confirms the absence of oxygen functionalities on the untreated LDPE surface. Ar plasma treatment at 225 and 300 W resulted in broadening of the C 1s peak and the occurrence of peak 2 centered at 285.7 eV, which is attributed to β -shift of the carbon atom adjacent to a carboxyl group.^{7,19} Since neither carboxyl nor other carbon—oxygen bonds were observed in the C 1s and O 1s spectra of LDPE treated at 225 and 300 W, peak 2 is assigned to carbon radicals or dangling bonds resulting from the abstraction of H atoms by the bombarding Ar ions. The peaks corresponding to carbon

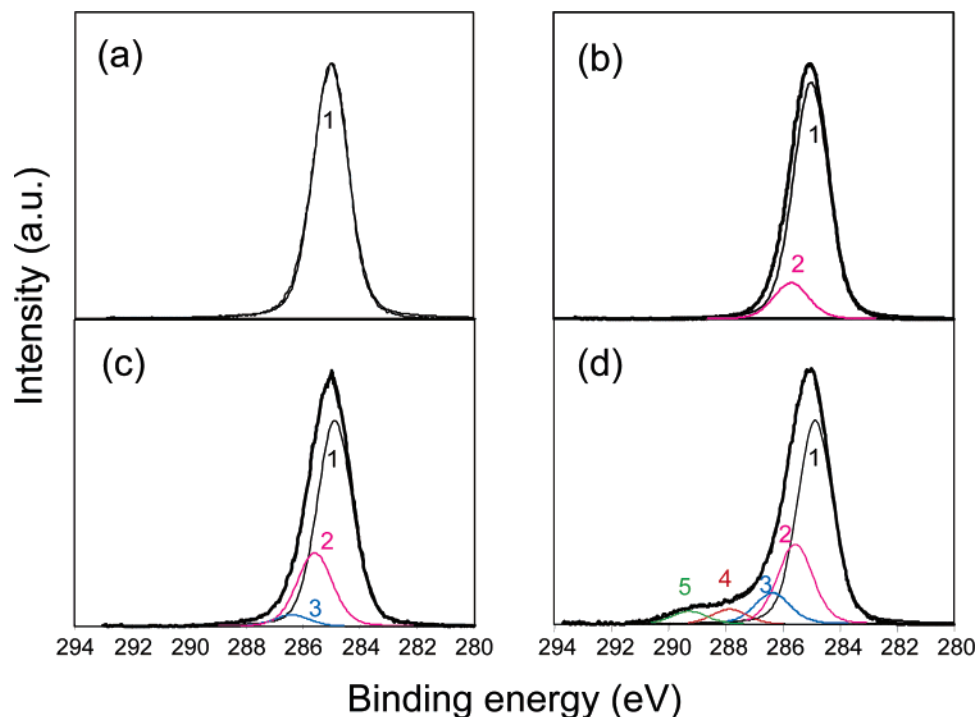


Figure 7. C 1s core level XPS spectra of LDPE with Gaussian-Lorentzian fits for plasma power equal to (a) 0 (untreated), (b) 225, (c) 375, and (d) 825 W.

TABLE 3: Effect of Plasma Power on Concentration of Carbon Functionalities in LDPE

plasma power (W)	concentration of carbon functionalities (at. %)			
	β -shift	C–O	C=O	O–C=O
0	0	0	0	0
225	18.6 ± 7.1	0	0	0
300	24.5 ± 5.9	0	0	0
375	27.2 ± 1.5	3.5 ± 0.6	0	0
450	26.5 ± 3.0	12.5 ± 3.0	4.6 ± 1.1	1.8 ± 0.5
825	26.5 ± 1.6	1.6 ± 1.8	4.5 ± 0.4	3.6 ± 0.4
1200	31.4 ± 2.1	12.2 ± 2.4	4.3 ± 0.6	2.5 ± 0.4

radicals and β -shift carbon atoms have the same binding energy. Increasing the plasma power from 225 to 375 W (i.e., ion energy fluence of 775 J/m^2) produced a new peak 3 centered at 286.5 eV, which is associated with alcohol and/or ether groups (C–O).^{3,11} The C 1s spectrum shown in Figure 7c is similar to that obtained in a previous study of Ar CCP discharge.²⁰ A very small O 1s peak (indistinguishable in the survey scan) was also observed in the spectrum of the 375 W plasma treatment. The presence of small amounts of oxygen on the LDPE surface treated at 375 W is in agreement with the decrease of the water contact angle from 82 to 75° with the increase of the plasma power from 300 to 375 W (Figure 5). Hence, this marked decrease in the water contact angle can be attributed to the formation of alcohol and/or ether functionalities for ion energy fluence equal to 775 J/m^2 .

Two additional peaks (4 and 5) appeared in the C 1s spectra of LDPE treated at a plasma power higher than 450 W. Figure 7d shows the C 1s spectrum of LDPE treated at 825 W, which, in addition to the previously discussed peaks 1–3, contains peaks 4 and 5 centered at binding energies equal to 288 and 289.3 eV, respectively. Peak 4 is assigned to carbonyl groups (C=O)^{3,11} and peak 5 to ester and/or carboxyl groups (O–C=O).³ Table 3 gives the atomic fraction of the polar carbon functionalities shown in Figure 7. All β -shift, C–O, C=O, and O–C=O functionalities were observed in the spectra of LDPE treated at a power higher than 450 W (i.e., ion energy fluence

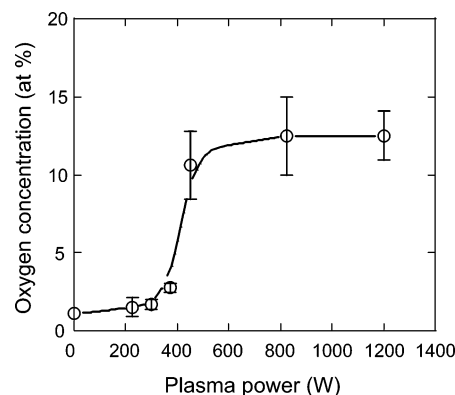


Figure 8. Effect of plasma power on oxygen concentration in LDPE.

higher than 2500 J/m^2). However, the fact that the fraction of these functionalities does not vary statistically above 450 W (Table 3) indicates that saturation commenced above the ion energy fluence threshold of 2500 J/m^2 .

Figure 8 shows the variation of the oxygen concentration (eq 4) with the plasma power. A relatively low oxygen concentration (~ 1.0 at. %) was obtained for plasma power less than 400 W (CCP discharge). An abrupt increase in oxygen concentration occurred when the plasma power increased to 450 W (2500 J/m^2), followed by a steady-state (12–13 at. %) above 450 W (ICP discharge). This trend is in agreement with the formation of β -shift, C–O, C=O, and O–C=O functionalities at power levels above 450 W discussed previously. Considering the evolution of these functionalities in terms of the ion energy fluence (Figure 2), it may be inferred that the critical energy fluence for high oxygen concentration (> 10 at. %) is 2500 J/m^2 .

The results shown in Figures 5–8 indicate that the main reason for the increase of the atomic oxygen concentration and the enhancement of the surface hydrophilicity, both observed above 450 W, was the development of C–O, C=O, and O–C=O polar functionalities, while the effect of β -shift carbon on the surface energy and chemistry change was secondary. These

functionalities are identical to those reported in previous studies dealing with different surface modification methods, such as oxygen plasma⁴ and corona discharge.⁷ Therefore, downstream ICP treatment with Ar can be used as an alternative method to oxygen plasma or corona discharge treatments to modify the surface chemistry of polymers with the added benefit of negligible physical changes, evidenced from the modification of the surface topography only at the nanoscale (nanotexturing).

It has been argued that the surface functionalities produced on polymer surfaces treated with oxygen plasma cannot be obtained with Ar plasma.^{4,17,30–32} Chemical reaction of polymer surfaces with Ar plasma involves the abstraction of hydrogen atoms and the subsequent formation of carbon radicals.¹⁷ These carbon radicals react with oxygen from the atmosphere to produce peroxy radicals and hydroperoxides,⁴ hence resulting in the formation of alcohol, ether, carbonyl, ester, and carboxyl groups. The results of this study show that the development of β -shift, C–O, C=O, and O–C=O functionalities is controlled by the ion energy fluence applied to the LDPE surface. For ion energy fluence less than 300 J/m² (CCP discharge), only β -shift carbon was observed on the LDPE surfaces (Table 3). These carbon radicals are not conducive to the formation of oxygen functionalities because their low energetic state does not promote reaction with oxygen. For ion energy fluence above 775 J/m², the oxygen concentration increased as a result of the formation of C–O groups, and increased further at higher ion energy levels (>2500 J/m²) due to the development of carbon radicals containing C=O and O–C=O groups (ICP discharge). Hence, by variation of the ion energy fluence, different physical (nanoscale) and chemical modifications were produced on LDPE surfaces.

Conclusions

Both chemical and physical modifications of LDPE surfaces were achieved by inductively coupled Ar plasma treatment. Different modifications were obtained by varying the rf power in the range of 75–1200 W. The results were interpreted in terms of the ion energy fluence determined from the ion density measured in situ with a Langmuir probe. At relatively low power (i.e., less than 400 W), the plasma was sustained by capacitively coupling (CCP discharge) and the ion energy fluence (<775 J/m²) applied to the LDPE surface was not sufficient to produce any physical or chemical changes. For a plasma power above 450 W (i.e., ion energy fluence higher than 2500 J/m²), the plasma was sustained by inductively coupling. Under the conditions of ICP discharge, the high ion energy resulted in chemical surface modifications characterized by the development of four polar functionalities, i.e., β -shift, C–O, C=O, and O–C=O. AFM analysis revealed that physical surface modification by ICP discharge involved only nanoscale topography changes, confirming that the conditions of downstream ICP discharge were not conducive to microscale roughening and/or etching of the LDPE surface. Contact angle and XPS measurements revealed that the hydrophilicity and surface chemistry of the treated LDPE were similar to those obtained with oxygen plasma under CCP discharge conditions.

The results of this study demonstrate that downstream ICP treatment with Ar is an effective method for producing polar functionalities that increase the surface energy and adhesion of polymers with negligible physical changes and surface damage. Therefore, the present technique can be used as an alternate

method to oxygen plasma treatment to minimize surface degradation. It was demonstrated that the nanoscale surface topography, hydrophilic behavior, and chemical properties of polyethylene can be altered in a controlled fashion by varying the ion energy fluence under conditions conducive to the sustainability of ICP discharge.

Acknowledgment. This work was funded by the National Science Foundation under Grant No. CMS-0085156. The authors are grateful to Professor M. A. Lieberman (University of California at Berkeley) for many helpful discussions on plasma physics, and Dr. E. J. Tonnis (Litmas Inc.) and D. Webb (Vacua Techniques) for technical assistance during the construction of the plasma treatment system.

References and Notes

- (1) Caldwell, R. A.; Woodell, J. E.; Ho, S. P.; Shalaby, S. W.; Boland, T.; Langan, E. M.; LaBerge, M. *J. Biomed. Mater. Res.* **2002**, *62*, 514.
- (2) Yasuda, H.; Sharma, A. K.; Yasuda, T. *J. Polym. Sci.: Polym. Phys. Ed.* **1981**, *19*, 1285.
- (3) Liston, E. M.; Martinu, L.; Wertheimer, M. R. *J. Adhes. Sci. Technol.* **1993**, *7*, 1091.
- (4) Kim, K. S.; Ryu, C. M.; Park, C. S.; Sur, G. S.; Park, C. E. *Polymer* **2003**, *44*, 6287.
- (5) Hoffman, A. S. *Adv. Polym. Sci.* **1984**, *57*, 141.
- (6) Dadbin, S.; Frounchi, M.; Saeid, M. H.; Gangi, F. *J. Appl. Polym. Sci.* **2002**, *86*, 1959.
- (7) Briggs, D.; Brewis, D. M.; Dahm, R. H.; Fletcher, I. W. *Surf. Interface Anal.* **2003**, *35*, 156.
- (8) Schönherr, H.; Vancso, G. J. *J. Polym. Sci., Part B: Polym. Phys.* **1998**, *36*, 2483.
- (9) Catoire, B.; Bouriot, P.; Demuth, O.; Baszkin, A.; Chevrier, M. *Polymer* **1984**, *25*, 766.
- (10) Marmieri, G.; Pettenati, M.; Cassinelli, C.; Morra, M. *J. Biomed. Mater. Res.* **1996**, *33*, 29.
- (11) Cho, C. K.; Kim, B. K.; Cho, K.; Park, C. E. *J. Adhes. Sci. Technol.* **2000**, *14*, 1071.
- (12) Komvopoulos, K. *J. Mech. Med. Biol.* **2001**, *1*, 17.
- (13) Klapperich, C.; Pruitt, L.; Komvopoulos, K. *J. Mater. Sci.: Mater. Med.* **2001**, *12*, 549.
- (14) Kim, B. K.; Kim, K. S.; Cho, K.; Park, C. E. *J. Adhes. Sci. Technol.* **2001**, *15*, 1805.
- (15) Blais, P.; Carlsson, D. J.; Csullog, G. W.; Wiles, D. M. *J. Colloid Interface Sci.* **1974**, *47*, 636.
- (16) Mittal, K. L. *Microscopic Aspects of Adhesion and Lubrication. Tribology Series 7*; Georges, J. M., Ed.; Elsevier: New York, 1982; p 153.
- (17) Clouet, F.; Shi, M. K. *J. Appl. Polym. Sci.* **1992**, *46*, 1955.
- (18) Yao, Y.; Liu, X.; Zhu, Y. *J. Adhes. Sci. Technol.* **1993**, *7*, 63.
- (19) France, R. M.; Short, R. D. *J. Chem. Soc., Faraday Trans.* **1997**, *93*, 3173.
- (20) Yasuda, H. *J. Macromol. Sci.—Chem. A* **1976**, *10*, 383.
- (21) Momose, Y.; Tamura, Y.; Ogino, M.; Okazaki, S.; Hirayama, M. *J. Vac. Sci. Technol. A* **1992**, *10*, 229.
- (22) Wu, J. Z.; Kang, E. T.; Neoh, K. G.; Wu, P.-L.; Liaw, D. J. *J. Appl. Polym. Sci.* **2001**, *80*, 1526.
- (23) Lieberman, M. A.; Lichtenberg, A. J. *Principles of Plasma Discharges and Materials Processing*; Wiley: New York, 1994; Chapters 6, 10, and 12.
- (24) Popov, O. A. *High Density Plasma Sources*; Noyes: Park Ridge, NJ, 1995.
- (25) Tonnis, E. J.; Graves, D. B.; Vartanian, V. H.; Beu, L.; Lii, T.; Jewett, R. *J. Vac. Sci. Technol. A* **2000**, *18*, 393.
- (26) Wagner, C. D.; Davis, L. E.; Zeller, M. V.; Taylor, J. A.; Raymond, R. H.; Gale, L. H. *Surf. Interface Anal.* **1981**, *3*, 211.
- (27) Hopwood, J.; Guarnieri, C. R.; Whitehair, S. J.; Cuomo, J. J. *J. Vac. Sci. Technol. A* **1993**, *11*, 152.
- (28) Denneman, J. W. *J. Phys. D: Appl. Phys.* **1990**, *23*, 293.
- (29) Van der Mei, H. C.; Stokroos, I.; Schakenraad, J. M.; Busscher, H. J. *J. Adhes. Sci. Technol.* **1991**, *5*, 757.
- (30) Briggs, D.; Seah, M. P. *Practical Surface Analysis. Auger and X-ray Photoelectron Spectroscopy*; Wiley: Chichester, U.K., 1983.
- (31) Kuzuya, M.; Niwa, J.; Ito, H. *Macromolecules* **1993**, *26*, 1990.
- (32) Retzko, I.; Friedrich, J. F.; Lippitz, A.; Unger, W. E. S. *J. Electron Spectrosc. Relat. Phenom.* **2001**, *121*, 111.